Lipidomic profiling reveals protective function of fatty acid oxidation in cocaine-induced hepatotoxicity[S]

Xiaolei Shi, Dan Yao, Blake A. Gosnell, and Chi Chen[1]

Department of Food Science and Nutrition, University of Minnesota, St. Paul, MN 55108

Abstract **During cocaine-induced hepatotoxicity, lipid accumulation occurs prior to necrotic cell death in the liver. However, the exact influences of cocaine on the homeostasis of lipid metabolism remain largely unknown. In this study, the progression of subacute hepatotoxicity, including centrilobular necrosis in the liver and elevation of transaminase activity in serum, was observed in a three-day cocaine treatment, accompanying the disruption of triacylglycerol (TAG) turnover. Serum TAG level increased on day 1 of cocaine treatment but remained unchanged afterwards. In contrast, hepatic TAG level was elevated continuously during three days of cocaine treatment and was better correlated with the development of hepatotoxicity. Lipidomic analyses of serum and liver samples revealed time-dependent separation of the control and cocaine-treated mice in multivariate models, which was due to the accumulation of long-chain acylcarnitines together with the disturbances of many bioactive phospholipid species in the cocaine-treated mice. An in vitro function assay confirmed the progressive inhibition of mitochondrial fatty acid oxidation after the cocaine treatment. Cotreatment of fenofibrate significantly increased the expression of peroxisome proliferator-activated receptor α (PPARα)-targeted genes and the mitochondrial fatty acid oxidation activity in the cocaine-treated mice, resulting in the inhibition of cocaine-induced acylcarnitine accumulation and other hepatotoxic effects. Overall, the results from this lipidomics-guided study revealed that the inhibition of fatty acid oxidation plays an important role in cocaine-induced liver injury.**—Shi, X., D. Yao, B. A. Gosnell, and C. Chen. **Lipidomic profiling reveals protective function of fatty acid oxidation in cocaine-induced hepatotoxicity.** ***J. Lipid Res.*** **2012.** 53: **2318–2330.**

Supplementary key words acylcarnitine • fenofibrate • peroxisome proliferator-activated receptor α

Cocaine, as one of the most widely abused psychological stimulants, is well known for causing addictive dependence and sudden death in its users (1). Besides its toxicity on the central nervous system (CNS) and the cardiovascular system (2, 3), cocaine causes liver injury in human and animal models (4–8). As diminished liver function contributes to various adverse health effects, including the dysfunction of CNS and cardiovascular system and the disruption of intermediary metabolism, cocaine-induced hepatotoxicity has been linked to the mortality in cocaine abusers (9, 10). Previous investigations of cocaine-elicited pathological and metabolic changes in animal models have yielded important insights on the initiation and development of cocaine-induced liver injury (11–13). First, biotransformation and bioactivation of cocaine and its metabolites are required to initiate cocaine-induced toxic events (14). Among those defined cocaine metabolism pathways, the hydrolysis reactions produce relatively nontoxic metabolites, whereas cytochrome P450 (P450) and flavin-containing monooxygenases (FMO)-mediated *N*-demethylation and *N*-oxidation reactions are responsible for generating reactive metabolites, such as *N*-hydroxynorcocoaine and norcocaine nitroxide. Second, oxidative stress-related events, including covalent binding to proteins (15), glutathione depletion (16), and lipid peroxidation (17), occur in the cocaine-treated liver, although their roles in cocaine-induced hepatotoxicity are not fully defined. Lastly, the disruption of normal function of mitochondria and other intracellular organelles as well as the dysregulation of signaling pathways in cell death

This work was supported by National Institutes of Health Grant 5R21DA-027469 (to C.C.). Its contents are solely the responsibility of the authors and do not necessarily represent the official views of the National Institutes of Health.

Manuscript received 22 April 2012 and in revised form 2 August 2012.

Published, JLR Papers in Press, August 19, 2012
DOI 10.1194/jlr.M027656

Abbreviations: Acot1, acyl-CoA thioesterase 1; ALT, alanine aminotransferase; AST, aspartate aminotransferase; BE, benzoylecgonine; BNE, benzoylnorecgonine; CMC, carboxymethyl cellulose; CNO, cocaine *N*-oxide; CNS, central nervous system; Coc, cocaine; Cpt1a, carnitine palmitoyltransferase 1a; Cpt2, carnitine palmitoyltransferase 2; CTL, control; EME, ecgonine methyl ester; FMO, flavin-containing monooxygenase; H&E, hematoxylin and eosin; LPC, lysophosphatidylcholine; LPE, lysophosphatidylethanolamine; MDA, multivariate data analysis; NCOC, norcocaine; NEME, norecgonine methyl ester; NOHBNE, *N*-hydroxybenzoylnorecgonine; OC, oleoylcarnitine; OHBE, hydroxybenzoylecgonine; OPLS, orthogonal PLS; P450, cytochrome P450; PalC, palmitoylcarnitine; PC, phosphatidylcholine; PCA, principal components analysis; PE, phosphatidylethanolamine; PLS-DA, projection to latent structures-discriminant analysis; PPARα, peroxisome proliferator-activated receptor alpha; RT, retention time; SC, stearoylcarnitine; SIC, single ion count; TAG, triacylglycerol; TBARS, thiobarbituric acid reactive substances; TIC, total ion count; UPLC, ultra-performance liquid chromatography; TOF-MS, time-of-flight mass spectrometry.

[1]To whom correspondence should be addressed.
e-mail: chichen@umn.edu

[S] The online version of this article (available at http://www.jlr.org) contains supplementary data in the form of one table and six figures.

and survival leads to progressive necrosis and apoptosis of hepatocytes (18–20).

Although previous studies have yielded multifaceted mechanistic information on cocaine-induced hepatotoxicity, our current understanding on this toxic event still remains insufficient. For example, the correlation between the metabolic events and the progression of cocaine-induced liver injury has not been extensively examined, even though the liver is the most important metabolic organ in the body. This situation is caused mainly by the limited analytical capacity and discovery power of the traditional targeted metabolite analysis approach. However, the developments in metabolomics and lipidomics have provided an alternative technical platform for examining the metabolic flux in a complex biomatrix through the combination of advanced analytical instrumentation and chemometric computation (21–23). The indiscriminant and untargeted nature of metabolomic and lipidomic analyses have led to the identification of novel biomarkers that guided subsequent mechanistic investigations of diseases and chemical-induced toxicities (24–26). In fact, a recent metabolomics-based study has revealed the potential role of tryptophan and purine metabolism in cocaine addiction (27).

In this study, the influences of cocaine treatment on the chemical composition of mouse serum and liver were investigated by the LC-MS-based lipidomic analysis. Biomarkers originated from the cocaine-induced disruption of fatty acid metabolism were further characterized. Cotreatment of fenofibrate, an activator of peroxisome proliferator-activated receptor α (PPARα), was performed to investigate the role of fatty acid oxidation in cocaine-induced liver injury.

EXPERIMENTAL PROCEDURES

Reagents

Palmitoylcarnitine, [$^{13}C_4$]palmitoylcarnitine, fenofibrate, carboxymethyl cellulose (CMC), 2-thiobarbituric acid, trichloroacetic acid, n-butanol, HPLC-grade water, acetonitrile, and formic acid were purchased from Sigma-Aldrich (St. Louis, MO). Cocaine, norcocaine, and benzoylecgonine were kindly supplied by RTI International (Research Triangle Park, NC) via the National Institute on Drug Abuse Drug Supply Program. CoA was purchased from MP Biomedicals (Santa Ana, CA). Triton X-100 was purchased from Alfa Aesar (Ward Hill, MA). Malondialdehyde bis (dimethyl acetal) was purchased from Acros Organics (Morris Plains, NJ). TRIzol reagent, SuperScript III Reverse Transcriptase kit, and SYBR green PCR master mix were purchased from Life Technologies (Carlsbad, CA).

Animal treatment and sample collection

Male C57BL/6 mice, 10–12 weeks old, were used in this study (28). All animals were maintained in a University of Minnesota (UMN) animal facility under a standard 12 h light/12 h dark cycle with food and water ad libitum. Handling and treatment procedures were in accordance with animal study protocols approved by the UMN Animal Care and Use Committee.

For cocaine treatment, cocaine was dissolved in a saline solution and administered at a dose of 30 mg/kg by daily intraperitoneal injection for three consecutive days. For fenofibrate treatment, fenofibrate was suspended in a 0.5% CMC solution and administered daily at a dose of 50 mg/kg by gavage. For cocaine and fenofibrate cotreatment, fenofibrate was administered 2 h earlier than cocaine on days 1, 2, and 3 of cocaine treatment. The control mice were treated with blank saline solution or CMC solution. Serum samples were collected by submandibular bleeding prior to treatment and at the end of each day of cocaine treatment, and urine samples were obtained by housing mice individually in metabolic cages for 24 h. Liver and other tissue samples were harvested after carbon dioxide euthanasia. All tissues samples were stored at −80°C before further analysis, except for small aliquots of liver tissue for histology.

Assessment of cocaine-induced toxicity

Fresh live tissues were immediately fixed, embedded, sectioned, and stained with hematoxylin and eosin (H&E) for general histology and with Oil Red O for lipid droplets. Cocaine-induced liver injury was evaluated by measuring serum alanine aminotransferase (ALT) and aspartate aminotransferase (AST) activities (Pointe Scientific, Canton, MI). Cocaine-elicited disruption of fatty acid metabolism was evaluated by measuring the levels of serum and hepatic triacylglycerol (TAG) using a colorimetric assay kit (Pointe Scientific). The status of lipid peroxidation was determined by thiobarbituric acid reactive substances (TBARS) assay using liver homogenates (29). Briefly, 50 mg liver was homogenized in 500 µl of 10 mM phosphate buffered solution (pH = 7.4) containing 1% (v/v) Triton X-100. After mixing 100 µl of liver homogenate with 200 µl of ice-cold 10% trichloroacetic acid, 200 µl of supernatant was obtained by centrifuging at 2,200 *g* for 15 min at 4°C, and then incubated with an equal volume of 0.67% (w/v) thiobarbituric acid for 10 min in a boiling water bath. The concentration of malondialdehyde was determined at 532 nm using a SpectraMax 250 spectrometer (Molecular Device, Sunnyvale, CA).

Preparation of serum and liver lipid extraction for LC-MS analysis

Deproteinization of serum was conducted by mixing one volume of serum with 19 vol of 66% aqueous acetonitrile and then centrifuging at 18,000 *g* for 10 min. Hepatic lipids were extracted from the liver based on the principle of Bligh and Dyer method (30). Liver samples (100 mg) were homogenized in 0.5 ml methanol and mixed with 0.5 ml chloroform and 0.4 ml water. Phase separation was achieved by 10 min centrifugation at 18,000 *g*. Lipid fraction in the chloroform phase was dried under nitrogen and then reconstituted in 0.5 ml n-butanol.

LC-MS analysis of serum and lipid extract

A 5 µl aliquot of diluted serum or liver lipid sample was injected into an Acquity UPLC system (Waters, Milford, MA) and separated by a gradient of mobile phase ranging from water to 95% aqueous acetonitrile containing 0.1% formic acid over a 10 min run. LC eluant was introduced into a SYNAPT QTOF mass spectrometer (Waters) for accurate mass measurement and ion counting. Capillary voltage and cone voltage for electrospray ionization (ESI) was maintained at 3 kV and 30 V for positive-mode detection, or at −3 kV and −35 V for negative-mode detection, respectively. Source temperature and desolvation temperature were set at 120°C and 350°C, respectively. Nitrogen was used as both cone gas (50 L/h) and desolvation gas (600 L/h), and argon as collision gas. For accurate mass measurement, the mass spectrometer was calibrated with sodium formate solution (range *m/z* 50–1,000) and monitored by the intermittent injection of the lock mass leucine enkephalin ($[M+H]^+$ = *m/z* 556.2771 and $[M+H]^-$ = *m/z* 554.2615) in real time. Mass chromatograms and mass spectral data were acquired and processed by MassLynx software (Waters) in centroided format. Additional structural information was

obtained tandem MS (MS/MS) fragmentation with collision energies ranging from 15 to 30 eV.

Chemometric analysis and biomarker identification

Chromatographic and spectral data of serum samples were deconvoluted by MarkerLynx software (Waters). A multivariate data matrix containing information on sample identity, ion identity [retention time (RT) and *m/z*], and ion abundance was generated through centroiding, deisotoping, filtering, peak recognition, and integration. The intensity of each ion was calculated by normalizing the single ion counts (SIC) versus the total ion counts (TIC) in the whole chromatogram. The data matrix was further exported into SIMCA-P+ software (Umetrics, Kinnelon, NJ) and transformed by mean-centering and *Pareto* scaling. Based on the complexity and quality of the data, either unsupervised or supervised multivariate data analysis (MDA), including principal components analysis (PCA) and projection to latent structures-discriminant analysis (PLS-DA), were adopted to analyze the serum and liver lipid data from control and cocaine-treated C57BL/6 mice. Major latent variables in the data matrix were described in a scores scatter plot of defined multivariate model. Potential biomarkers were identified by analyzing ions contributing to the principal components and to the separation of sample groups in a S-loadings plot of orthogonal PLS (OPLS) discriminant analysis (22, 31). The chemical identities of biomarkers were determined by accurate mass measurement, elemental composition analysis, database search (Lipid Maps: http://www.lipidmaps.org/, Human Metabolome Database: http://www.hmdb.ca/), MS/MS fragmentation, and comparisons with authentic standards if available.

Quantitation of palmitoylcarnitine in serum and liver

Palmitoylcarnitine (PalC) in serum and liver lipid extracts was quantified by accurate mass-based ion extraction chromatograms. Stable isotope-labeled PalC ([$^{13}C_4$]PalC) was used as the internal standard. PalC concentrations were determined by calculating the ratio between the peak area of PalC and the peak area of [$^{13}C_4$]PalC and fitting with a standard curve with a linear range from 10 nM to 1 μM ($r = 0.99$) using QuanLynx software (Waters).

In vitro assay of hepatic mitochondrial β-oxidation activity

Hepatic mitochondrial β-oxidation activity was evaluated by the rate of PalC utilization (32). Mitochondria were isolated from the liver by differential centrifugation (33). Incubations of 20 μM PalC with 0.5 mg/kg liver mitochondria homogenate were then carried out in a Tris-HCl buffer containing 0.05% Triton X-100, 10 mM $MgCl_2$, and 1 mM CoASH in a final volume of 200 μl for 15 min at 37°C. The reactions were terminated by adding 400 μl acetonitrile. The rate of PalC utilization was calculated based on the LC-MS quantitation of PalC concentration after the incubation.

Profiling cocaine metabolism in mouse

The profile of cocaine metabolism was determined by LC-MS analysis of cocaine metabolites in the urine. Details of the identification and structural elucidation of cocaine metabolite will be described in a separate report. Briefly, the chromatographic peaks of all identified urinary cocaine metabolites were identified, and their peak areas were determined using accurate mass measurement-based MetaboLynx software (Waters) (34). The profiles of urinary cocaine metabolites during three-day cocaine treatment were compared by calculating the percentage of the peak area of each single metabolite in the pooled total peak area (area % ± SD) of cocaine metabolites.

Gene expression analysis

Total RNA was extracted from the livers of C57BL/6 mice using TRIzol reagent. Quantitative real-time PCR (qPCR) was performed using cDNA generated from 1 mg total RNA with SuperScript III Reverse Transcriptase. Primers were designed using NCBI/Primer-BLAST (http://www.ncbi.nlm.nih.gov/tools/primer-blast/), and sequences are enlisted in supplementary Table I. qPCR reactions were carried out using SYBR green PCR master mix with a StepOnePlus system (Applied Biosystems). Gene expression levels were quantified using the Comparative CT method and normalized to 18S rRNA.

Statistics

Experimental values are expressed as mean ± standard deviation (SD). Statistical analysis was performed with two-tailed Student *t*-tests for unpaired data, with $P < 0.05$ considered statistically significant.

RESULTS

Time course of cocaine-induced liver injury

To characterize the development of cocaine-induced hepatotoxicity, C57BL/6 mice were treated with 30 mg/kg of cocaine by intraperitoneal injection for three consecutive days. Microscopic examination of liver histology by H&E and Oil Red O staining revealed the progression of cocaine-induced liver injury (**Fig. 1A** and supplementary Fig. I-A). On day 1, hepatocytes were slightly swelling with increased vacuoles, but no clear cell death was observed. On day 2, hepatocytes in the centrilobular area appeared to be ballooning and started to lose nuclei, and enlarged lipid droplets became apparent. On day 3, necrotic hepatocytes were prevalent around the central vein along with inflammatory infiltration, and the development of microvesicular steatosis was evident in the surrounding cells (Fig. 1A and supplementary Fig. I-A). Consistent with the histological observation, serum ALT and AST activity remained unchanged on day 1 but dramatically increased on day 2 and 3 of cocaine treatment (Fig. 1B and supplementary Fig. I-B), which suggests that cocaine-induced damage on hepatocytes at this dose (30 mg/kg) is a subacute toxic event instead of an acute one. Based on the appearance of lipid vacuoles and vesicles in cocaine-treated liver, the degree of lipid accumulation was evaluated by measuring TAG in the liver and serum. Both liver and serum TAG levels increased significantly after just one dose of cocaine exposure. However, the serum TAG level remained largely unchanged after day 1, whereas the hepatic TAG level further increased dramatically on day 3 of treatment (Fig. 1C, D). Similar to the change in hepatic TAG level, the hepatosomatic index (ratio of liver weight/body weight) was also elevated on days 1 and 3 of cocaine treatment (Fig. 1E). Lipid peroxidation was examined by measuring TBARS content in the liver. The TBARS level peaked rapidly on day 1 of cocaine treatment, but it was not further increased afterwards (Fig. 1F). Overall, among all measured biochemical parameters, the increase of hepatic TAG on day 3 of cocaine treatment had the best correlation with the development of necrosis in the liver and the release of transaminase from the liver.

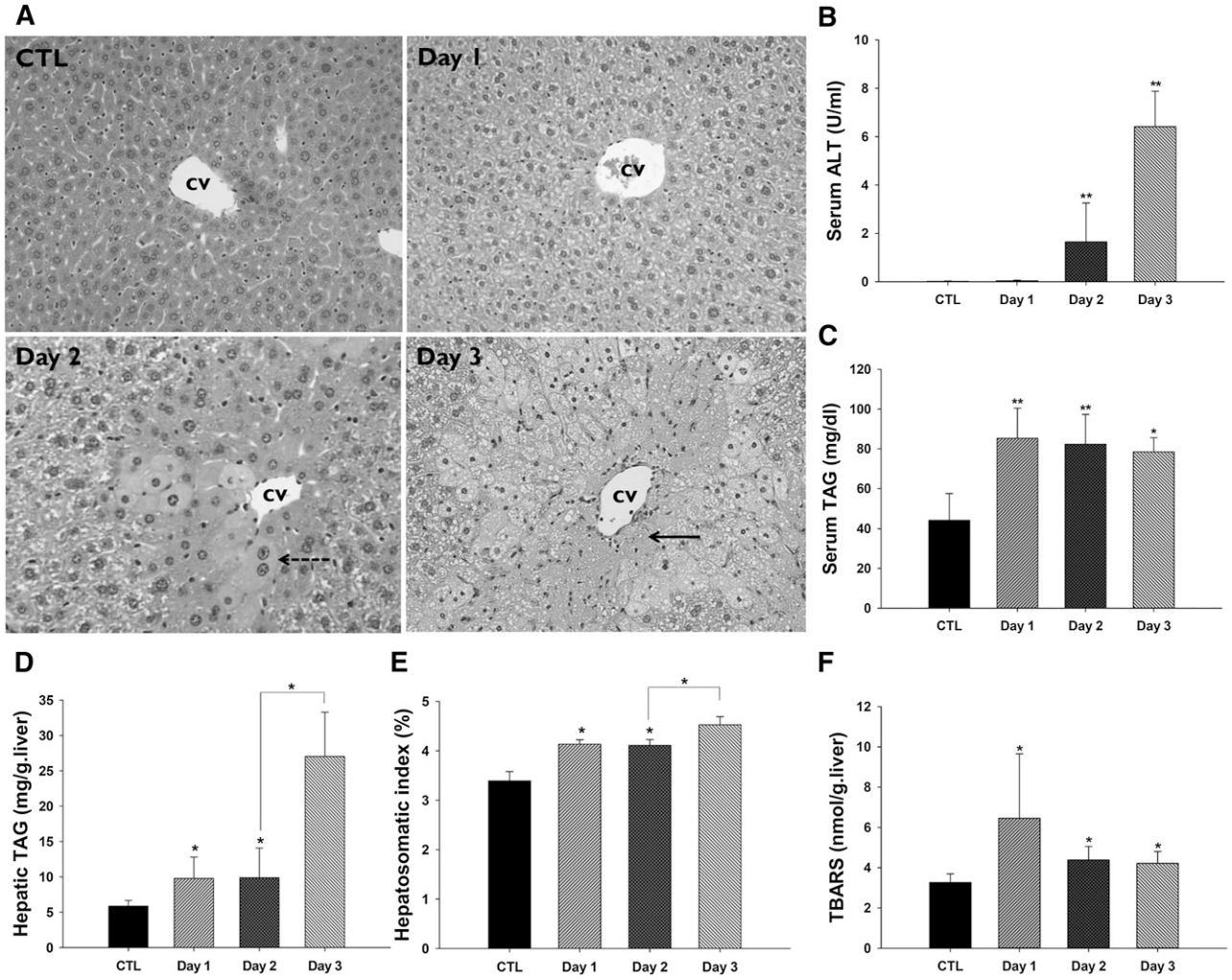

Fig. 1. Histological and biochemical analyses of the influence of cocaine treatment on the C57BL/6 mice. (A) Histology of the liver (magnification: 100×). The location of hepatic central vein (CV) was marked. Dash arrow points to ballooning hepatocytes; solid arrow points to necrotic hepatocytes. (B) Serum ALT activity. (C) TAG level in the serum. (D) TAG level in the liver. (E) Hepatosomatic index. (F) TBARS value in the liver. Values were presented as mean ± SD (n = 4–8). $*P < 0.05$ and $**P < 0.01$ indicate statistical significance between control and cocaine-treated samples or between specified pair of samples.

The stepwise changes in hepatic TAG level suggested that different metabolic events and mechanisms might contribute to the histological phenotypes and steatosis on days 1 and 3 of cocaine treatment.

Metabolomic investigation of cocaine-induced metabolic events

To further explore the metabolic events associated with subacute hepatotoxic effects of cocaine, especially the changes in the lipidome, serum samples and liver lipid extracts were examined through LC-MS-based lipidomic analysis. After the chromatographic and mass spectral data acquired from LC-MS analysis were processed by multivariate analysis, a two-component model represented by a scores scatter plot (**Fig. 2A**) was constructed to illustrate the relationship among sample groups. The distinctive separation of serum samples collected at the different time points of cocaine treatment (Fig. 2A) indicated that cocaine dramatically altered the chemical composition of serum in a time-dependent pattern, suggesting the existence of serum metabolites correlating to the development of cocaine-induced liver injury. Serum ions (I–XXII) contributing to the classification of cocaine and control groups were further identified in a loadings S-plot (Fig. 2B). The majority of identified biomarkers belong to the subfamilies of polar lipids, which are phosphatidylcholines (PC: III–XI, XIV, XXI), lysophosphatidylcholines (LPC: I, II, XII, XIII), phosphatidylethanolamine (PE: XXII), lysophosphatidylethanolamines (LPE: XVIII–XX), and acylcarnitines (XV–XVII) (**Table 1**). These identifications were made through accurate mass measurement; elemental composition analysis; MS/MS fragmentation; chromatographic and spectroscopic comparison with authentic standards; or published data in metabolomic and lipidomic databases. For example, palmitoylcarnitine (PalC, XVI) was identified through chromatographic and spectral comparisons with the authentic standard (Fig. 2C, D), whereas the structural moiety and fatty acid content of PC and PE molecules were elucidated through the interrogation of MS/MS spectra, even though the positions of acyl group in the glycerol backbone was

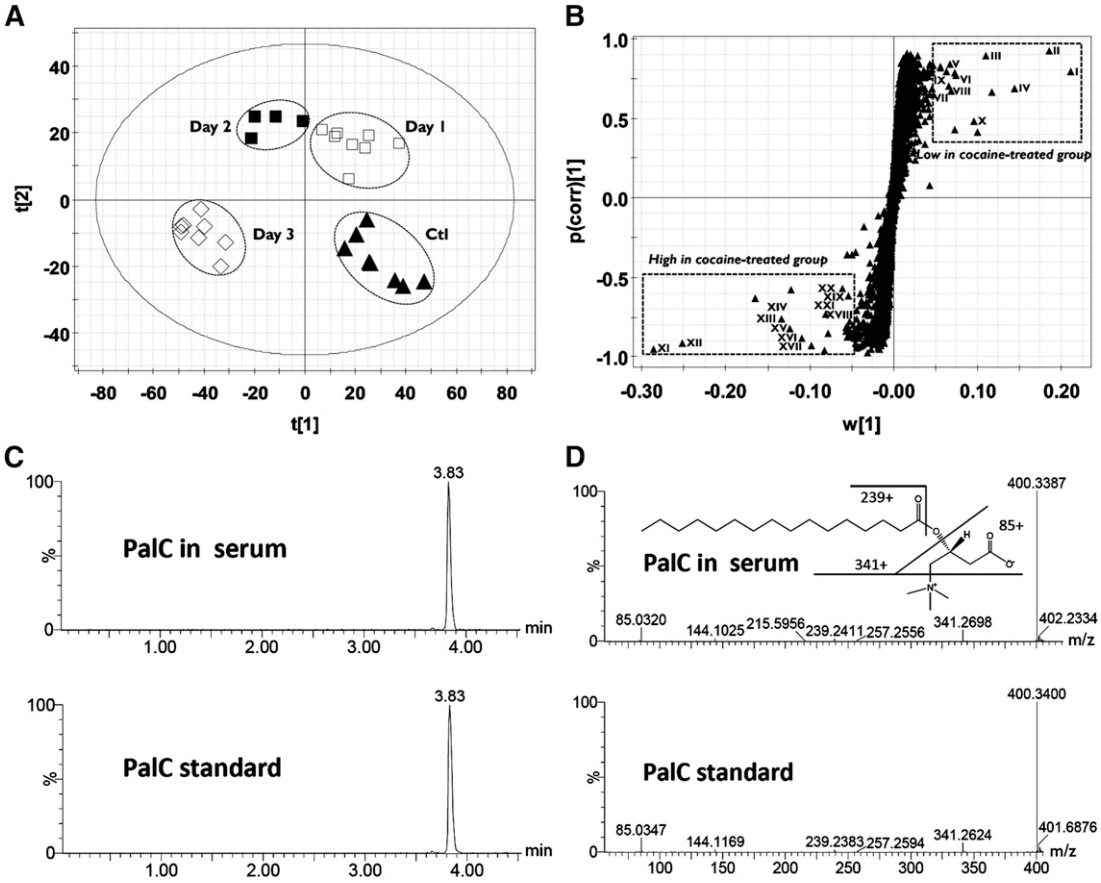

Fig. 2. Identification of serum metabolites altered by cocaine treatment through LC-MS-based metabolomics. Conditions of LC-MS measurement and procedures of data processing and analysis are described in Experimental Procedures. (A) The scores plot of a PLS-DA model on serum samples from the control mice [labeled as CTL (filled square)] and the mice treated with 30 mg/kg cocaine [labeled as day 1 (open square), day 2 (filled square), and day 3 (open diamond)] (n = 4–8). The $t[1]$ and $t[2]$ values represent the scores of each sample in the principal component 1 and 2, respectively. Fitness (R^2) and prediction power (Q^2) of this PLS-DA model are 0.82 and 0.41, respectively. (B) The S-loadings plot of serum ions contributing to the classification of serum samples. Major serum ions (I–XXII) interfered by cocaine treatment were labeled and their chemical identities were enlisted in Table 1. (C) The comparison between the chromatogram of serum PalC (XVI) and the chromatogram of PalC standard. (D) The representative MS/MS spectra of serum PalC (XVI) and PalC standard. The fragmentation pattern of PalC is interpreted in the inlaid diagram.

not resolved (supplementary Fig. II-A, B). Examination of their relative abundances in the detected MS signals of serum revealed several clear trends of changes in serum lipidome, which included the following. First, dramatic increase of long-chain acylcarnitines on days 2 and 3 of cocaine treatment, including PalC (XVI), oleoylcarnitine (OC; XVII), and stearoylcarnitine (SC; XV) (**Fig. 3A**). Second, the increase of LPC(16:0) (XII) and LPC(18:2) (XIII) but the decrease of LPC(20:4) (I) and LPC(20:3) (II) (Fig. 3B), suggesting that the elongation and desaturation of fatty acids in vivo were potentially reduced after cocaine treatment. This is further supported by the observation of the increase of PC(16:0/18:2) (XI) and PC(16:0/16:0) (XXI), which only contain 16- and 18-carbon fatty acids, and the decrease of PC(18:0/20:3) (III) and PC(18:1/22:6) (VI), which contain 20- and 22-carbon PUFAs (Fig. 3C). Third, the significant increase of LPE species on day 3 of cocaine treatment, including LPE(18:2) (XVIII), LPE(22:6) (XIX), and LPE(20:4) (XX) (Fig. 3D). Furthermore, the time-dependent separation among the control and cocaine-treated liver lipid extracts was observed following lipidomic analysis, and the lipid species contributing to the separation were similar to those identified through serum lipid analysis (supplementary Fig. III-A, B).

Influence of cocaine treatment on mitochondrial fatty acid oxidation in the liver

Among all identified changes in the lipidome (Figs. 2 and 3 and Table 1), the increase in the relative abundance of long-chain acylcarnitines is highly relevant to cocaine-induced hepatic steatosis due to their identity as specific substrates of mitochondrial β-oxidation. To validate this observation, the levels of PalC (XVI) in both serum and liver during the three-day cocaine treatment were quantified. The results showed that PalC in serum and liver remained unchanged on day 1 of cocaine treatment, was significantly elevated on day 2, and was dramatically increased on day 3 (**Fig. 4A**, B), indicating that acylcarnitine accumulated in the liver and was subsequently released into serum after cocaine treatment. The inhibition of fatty acid oxidation, as suggested by the accumulation of PalC, was further confirmed by the in vitro mitochondrial

TABLE 1. Serum metabolite markers after three-day cocaine treatment

Markers	RT (min)	$[M+H]^+$	Formula	Identity	Trend after Cocaine
I	4.20	544.3404	$C_{28}H_{50}NO_7P$	LPC (20:4)	↓
II	4.32	546.3564	$C_{28}H_{52}NO_7P$	LPC (20:3)	↓
III	7.21	812.6209	$C_{46}H_{86}NO_8P$	PC (18:0/20:3)	↓
IV	6.89	808.5884	$C_{46}H_{82}NO_8P$	PC (18:1/20:4)	↓
V	6.98	810.6056	$C_{46}H_{84}NO_8P$	PC (18:0/20:4)	↓
VI	6.83	832.5915	$C_{48}H_{82}NO_8P$	PC (18:1/22:6)	↓
VII	6.58	780.5577	$C_{44}H_{78}NO_8P$	PC (16:1/20:4)	↓
VIII	6.59	830.5742	$C_{48}H_{80}NO_8P$	PC (18:2/22:6)	↓
IX	6.59	854.5754	$C_{50}H_{80}NO_8P$	PC (20:4/22:6)	↓
X	6.81	782.5713	$C_{44}H_{80}NO_8P$	PC (16:0/20:4)	↓
XI	6.80	758.5711	$C_{42}H_{80}NO_8P$	PC (16:0/18:2)	↑
XII	4.26	496.3394	$C_{24}H_{50}NO_7P$	LPC (16:0)	↑
XIII	4.18	520.3398	$C_{26}H_{50}NO_7P$	LPC (18:2)	↑
XIV	7.12	786.6030	$C_{44}H_{84}NO_8P$	PC (18:0/18:2)	↑
XV	3.90	426.3545	$C_{25}H_{49}NO_4$	Stearoylcarnitine	↑
XVI	3.83	400.3412	$C_{23}H_{45}NO_4$	Palmitoylcarnitine	↑
XVII	3.74	424.3415	$C_{25}H_{47}NO_4$	Oleoylcarnitine	↑
XVIII	4.16	478.2953	$C_{23}H_{44}NO_7$	LPE(18:2)	↑
XIX	4.20	526.3018	$C_{27}H_{44}NO_7P$	LPE(22:6)	↑
XX	4.19	502.3119	$C_{25}H_{44}NO_7P$	LPE(20:4)	↑
XXI	6.93	734.5713	$C_{40}H_{80}NO_8P$	PC (16:0/16:0)	↑
XXII	6.74	764.5234	$C_{43}H_{74}NO_8P$	PE(16:0/22:6)	↑

The process of identifying serum metabolites responsive to cocaine treatment is described in Experimental Procedures. The most prominent markers revealed by the S-plot of OPLS model (labeled in Fig. 2B) were further investigated by accurate mass measurement, MS/MS fragmentation, and structural elucidation. Retention time (RT) of each marker was its elution time from a 10 min run in a C_{18} UPLC column. Fatty acid contents of phospholipids were determined by examining their MS/MS pattern, but their positions (*sn*-1 and *sn*-2) in PCs and PEs was not resolved. ↑, increased; ↓, decreased.

β-oxidation functional assay. The utilization of PalC by mitochondria was significantly reduced on day 3 compared with other time points (Fig. 4C).

Protective effects of fenofibrate on cocaine-induced liver injury

Fatty acid oxidation is mainly regulated by transcriptional factor PPARα (35). To examine the role of fatty acid oxidation in cocaine-induced hepatotoxicity, fenofibrate, a PPARα agonist, was fed to the mice on all three days of cocaine treatment. The results of H&E and Oil Red O staining clearly showed that fenofibrate cotreatment was highly protective against cocaine-induced histological changes in the centrilobular region of the liver, as evidenced by the lack of necrotic cells and microvesicular steatosis in the liver treated with both cocaine and fenofibrate (**Fig. 5A** and supplementary Fig. IV-A). Consistent with the histological findings, biochemical indices of cotreated mice, including ALT, AST, hepatosomatic index, and serum and hepatic TAG, remained in normal levels in contrast to the dramatic changes in the cocaine-alone mice (Fig. 5B–E and supplementary Fig. IV-B). This protective effect of fenofibrate was also confirmed by observing the decrease of cocaine-induced TBARS level in the liver (Fig. 5F). Therefore, concurrent fenofibrate treatment was highly effective in rescuing the liver from cocaine-induced steatosis and other histopathological changes. Moreover, the effects of treating with fenofibrate one day and two days after starting cocaine treatment were examined (supplementary Fig. VI-A). Even though not as effective as the concurrent cotreatment, the postcocaine administrations of fenofibrate were still able to partially and time-dependently reduce the elevation of serum aminotransferases (supplementary Fig. VI-B, C) induced by three-day cocaine treatment.

Cocaine metabolism during cocaine and fenofibrate treatments

As a versatile transcription factor, PPARα not only regulates enzymes and transporters important in lipid metabolism but also can affect many xenobiotic-metabolizing enzymes (36, 37). Because cocaine-induced hepatotoxicity is initiated by cocaine metabolism, especially the production of reactive cocaine metabolites, the effects of fenofibrate on cocaine metabolism were evaluated through LC-MS-based profiling of major urinary cocaine metabolites on days 1 and 3 of the treatments. The resulted showed that the levels of two reactive *N*-demethylation metabolites, benzoylnorecgonine (BNE) and norcocaine (NCOC), on day 3 were higher than their levels on day 1, whereas an opposite trend was observed for benzoylecogonine (BE) and *N*-hydroxybenzoylecogonine (OHBE), two nontoxic metabolites formed by the hydrolysis of cocaine (**Fig. 6**). These observations suggest that the bioactivation of cocaine was induced by itself. Compared with observed time-dependent differences, fenofibrate did not affect cocaine metabolism, because the cocaine metabolite profile in the cotreatment group was comparable to that in the cocaine-alone group on both day 1 and day 3 (Fig. 6). Therefore, the protective effects of fenofibrate on cocaine-induced liver injury were not due to the modification of cocaine metabolism.

Effects of fenofibrate on cocaine-induced changes in the lipidome

The lipidomic changes associated with the protective effects of fenofibrate were examined through LC-MS

JOURNAL OF LIPID RESEARCH ASBMB

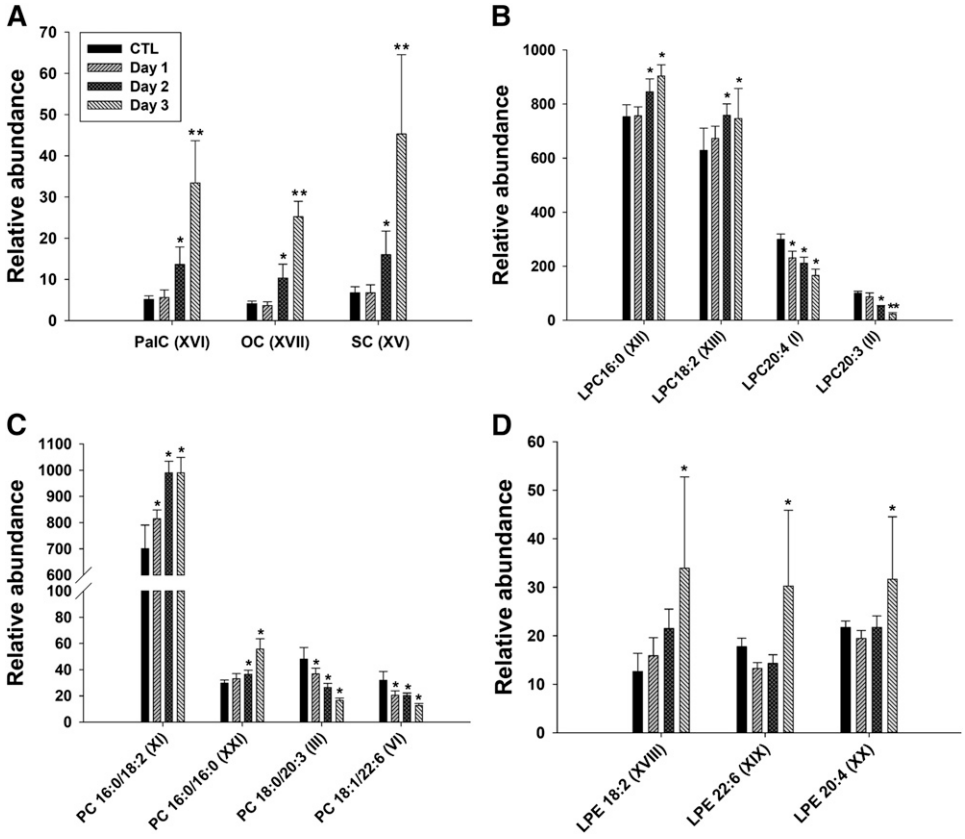

Fig. 3. Time-dependent changes in serum lipid species after three-day 30 mg/kg cocaine treatment. (A–D) Relative abundance of acylcarnitines, LPCs, PCs, and LPEs in the serum. Values were presented as mean ± SD (n = 4–8). *$P < 0.05$ and **$P < 0.01$ indicate statistical significance between control and cocaine-treated samples.

analysis of serum samples from fenofibrate-cocaine, cocaine-alone, fenofibrate-alone, and control treatments. The results showed distinctive separation of four sample groups in the scores scatter plot of a three component PLS-DA model (**Fig. 7A**). Besides expected differences between control and cocaine groups, the separation of the cotreatment group from the cocaine-alone group was also apparent, suggesting fenofibrate significantly altered the lipid composition of cocaine-treated mice. The serum ions contributing to the distinction of the cocaine group from the cotreatment and control groups were further characterized in an S-plot and labeled according to Table 1 (Fig. 7B). Examination of their relative abundances in serum revealed the protective effects of fenofibrate against the cocaine-induced alterations in the lipidome. For example, fenofibrate completely abolished the cocaine-induced acylcarnitine accumulation (Fig. 7C), and it also partially reversed the change in several LPC, PC, and LPE species (Fig. 7D). Furthermore, analyzing the liver lipids revealed similar separation among sample groups (supplementary Fig. V-A). Lipid species contributing to the separation were overlapping with ones identified in serum analysis (supplementary Fig. V-B).

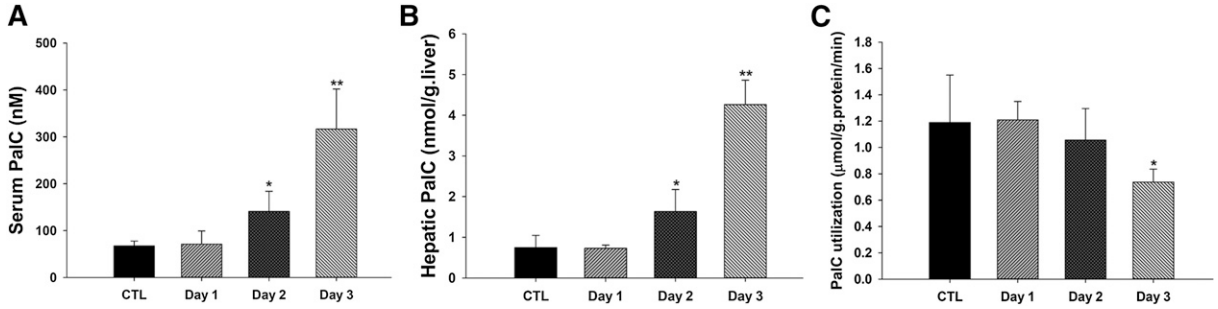

Fig. 4. Evaluation of mitochondrial β-oxidation function in the liver after three-day 30 mg/kg cocaine treatment. (A) PalC level in the serum. (B) PalC level in the liver. (C) Utilization of PalC in the liver. The in vitro β-oxidation functional assay is described in the Experimental Procedures. Values were presented as mean ± SD (n = 4–8). *$P < 0.05$ and **$P < 0.01$ indicate statistical significance between control and cocaine-treated samples.

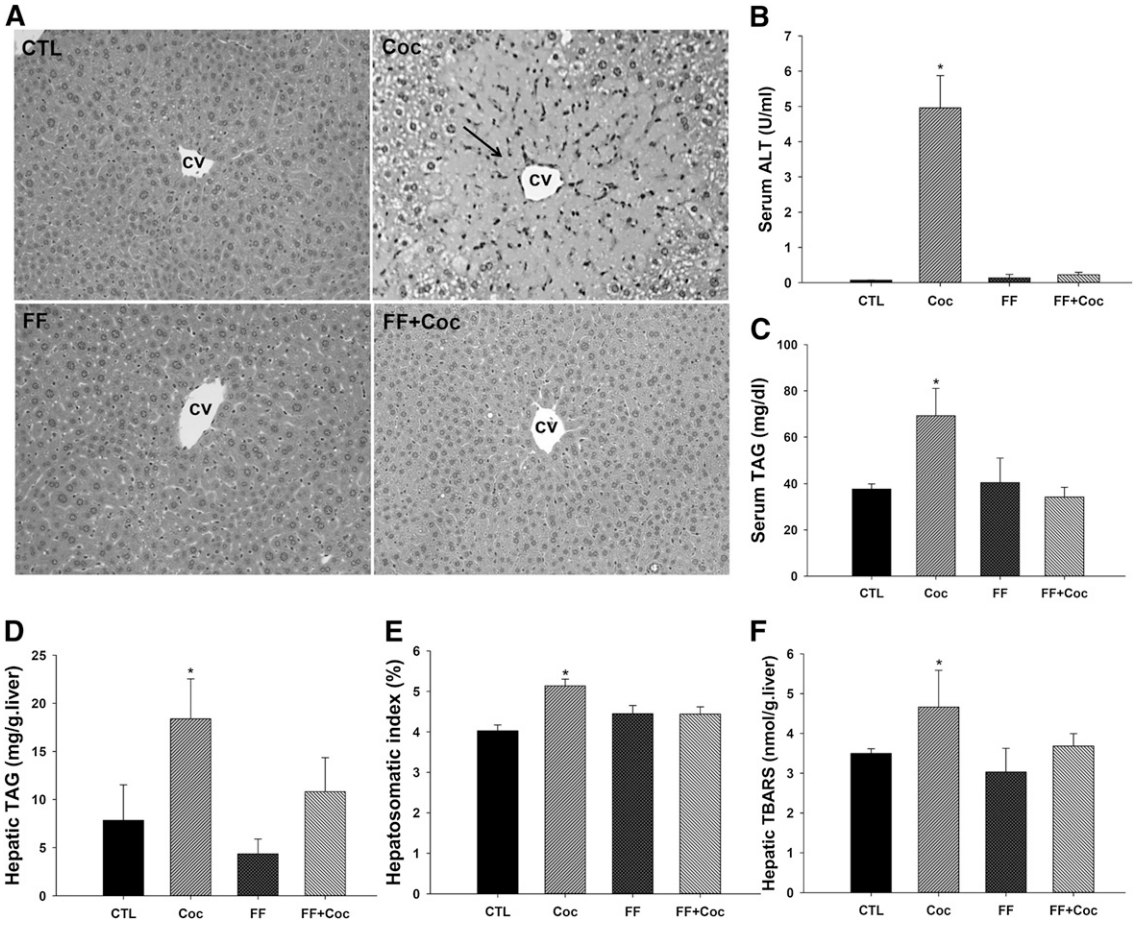

Fig. 5. Protective effects of fenofibrate against cocaine-induced hepatotoxicity in the C57BL/6 mice. The protocol of cotreatment of 50 mg/kg fenofibrate with 30 mg/kg cocaine for three days is described in Experimental Procedures. (A) Histology of the liver (magnification: 100×). The location of hepatic central vein (CV) was marked. Solid arrow points to necrotic hepatocytes. (B) Serum ALT activity. (C) TAG level in the serum. (D) TAG level in the liver. (E) Hepatosomatic index. (F) TBARS value in the liver. Values were presented as mean ± SD (n = 3–4). *$P < 0.05$ and **$P < 0.01$ indicate statistical significance between control and marked samples.

Effects of fenofibrate on cocaine-induced inhibition of mitochondrial β-oxidation function

Quantitative analysis of serum and hepatic PalC levels from the concurrent cotreatment and postcocaine treatments of fenofibrate was performed to validate the observations from the lipidomic analysis. The result showed that the concurrent cotreatment of fenofibrate with cocaine prevented the cocaine-induced increase of PalC in both serum and liver (**Fig. 8A**, B), and the postcocaine treatment of fenofibrate also partially and time-dependently reversed PalC accumulation (supplementary Fig. VI-D, E). The protective effect of fenofibrate was likely due to the preservation of mitochondrial β-oxidation function in cocaine-treated mice, as the mitochondrial utilization of PalC was sustained in the cotreated mice (Fig. 8C).

Effects of fenofibrate on PPARα-targeted genes

The influence of fenofibrate and cocaine on PPARα-targeted genes was further examined by measuring the expression of carnitine palmitoyltransferase 1a (*Cpt1a*), carnitine palmitoyltransferase 2 (*Cpt2*), and acyl-CoA thioesterase 1 (*Acot1*), three genes involving in mitochondrial β-oxidation and acyl-CoA turnover. As expected, fenofibrate treatment alone increased the expression of PPARα-targeted genes (**Fig. 9A**–C). The trend of upregulating PPARα activity was also observed from the cocaine-alone treatment (Fig. 9). The cotreatment of fenofibrate and cocaine led to the highest levels of gene expression of *Cpt1a*, *Cpt2*, and *Acot1* among all treatments (Fig. 9). This correlation between the activation of PPARα-targeted genes and the recovery of mitochondrial β-oxidation activity (Fig. 8C) suggested that the protective effect of fenofibrate against cocaine-induced lipid accumulation and hepatotoxicity was at least partially due to the PPARα-mediated upregulation of fatty acid oxidation. Furthermore, the results from the postcocaine administration of fenofibrate indicated that early activation of PPARα-targeted genes by fenofibrate (supplementary Fig. VI-F) was positively correlated with the protection against cocaine-induced liver injury.

DISCUSSION

Mechanisms of cocaine-induced liver injury have been studied for over three decades due to the stature of cocaine as one of the most harmful substances in modern society (1). Following the identification of reactive cocaine

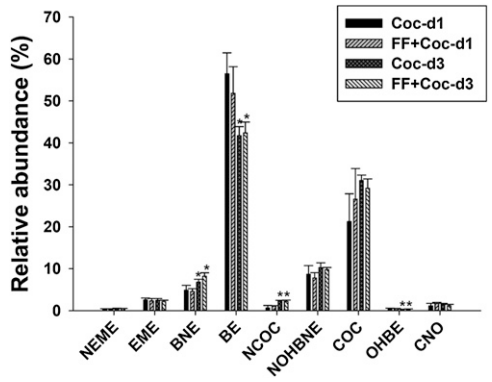

Fig. 6. Influence of repeated cocaine exposure and fenofibrate on cocaine metabolism. The procedure of determining the profile of urinary cocaine metabolites is described in Experimental Procedures. Relative abundances of cocaine and eight major urinary metabolites on days 1 and 3 of cocaine-alone treatment (30 mg/kg) and fenofibrate (50 mg/kg)-cocaine cotreatment were compared. Values were presented as mean ± SD (n = 3–4). $*P < 0.05$ indicates statistical significance between days 1 and 3.

metabolites, such as *N*-hydroxynorcocaine (38) and norcocaine nitroxide (39), the majority of mechanistic studies have focused on the bioactivation of cocaine as well as subsequent covalent protein binding and disruption of redox homeostasis, including glutathione depletion and lipid peroxidation. Results from these studies have clearly indicated that metabolic activation and oxidative stress are indispensable components of cocaine toxicity (11–13). However, the adverse effects of cocaine exposure are not limited to the direct interaction with cytoprotective and cytotoxic pathways. As a potent uptake inhibitor of catecholamines, cocaine, especially cocaine abuse, can dramatically increase norepinephrine and epinephrine levels in synapses and sympathetic nerve endings (40). Because adrenergic receptors, the physiological targets of catecholamines, are actively involved in the regulation of carbohydrate, amino acid, and lipid metabolism (41–44), cocaine is expected to significantly affect intermediary metabolism. Observed pathophysiological events, including the increase of lactate and basal metabolism rate (45, 46), as well as the elevation of cardiac output and blood pressure (48), support this assumption. However, the exact effects of cocaine exposure on intermediary metabolism remain largely unknown. In addition, the role of intermediary metabolism in cocaine-induced hepatotoxicity has not been explored.

Cocaine-induced fatty liver in animal and human has been reported previously (48–50). In this study, a new feature of fatty liver development in mouse following subacute treatment of cocaine was identified, i.e., hepatic TAG level increased on days 1 and 3 of cocaine treatment, respectively, whereas serum TAG level increased on day 1 but remained largely unchanged thereafter (Fig. 1C, D). Compared with serum TAG level, the two-stage induction of hepatic TAG was better correlated to the results of histological and biochemical analyses, which showed that apparent development of microvesicular steatosis and dramatic increase of transaminase activity mainly occurred after day 1 (Fig. 1A, B and supplementary Fig. I-A, B). Therefore, examining the causes underlying the increase of hepatic TAG level might provide insights on cocaine-induced hepatotoxicity. Hepatic TAG level is regulated by multiple processes in TAG turnover in the liver, which include import and biosynthesis of fatty acids, TAG synthesis, TAG hydrolysis, fatty acid utilization (mainly oxidation), and TAG secretion. In this study, metabolomic analysis revealed that long-chain acylcarnitine levels in serum and liver were well correlated to the progression of hepatotoxicity (Fig. 4A, B and Table 1), and the acylcarnitine accumulation in vivo was confirmed by observing reduced PalC utilization by the mitochondria from cocaine-treated liver (Fig. 4C), indicating that cocaine treatment caused significant compromise of mitochondrial β-oxidation function. Because of the importance of fatty acid oxidation in TAG turnover and energy metabolism, these results revealed a contributing mechanism for the development of microvesicular steatosis and liver toxicity in subacute cocaine treatment.

Mitochondrial dysfunction as a key component in cocaine toxicity has been investigated previously. Supporting evidence includes the observations of morphological alterations of hepatic mitochondria in mice after cocaine treatment and a dose- and time-dependent decrease of mitochondrial membrane potential (16, 51). A recent study using purified rat heart mitochondria also reported that cocaine inhibited octanoylcarnitine-mediated respiration (52). Identification of cocaine-elicited inhibition of hepatic β-oxidation in vivo in this study further underscores the importance of mitochondria in cocaine-induced hepatotoxicity. Besides cocaine, the inhibition of mitochondrial fatty acid oxidation has been identified as a major mechanism of the hepatotoxicity induced by many therapeutic agents and environmental toxicants, including acetaminophen (53), aspirin, and hypoglycin (54). The direct consequences of suppressed fatty acid oxidation function are the disruption of energy metabolism and the accumulation of TAG and fatty acids. These changes can further impact other metabolic events, as well as the susceptibility of hepatocytes to oxidative stress and chemical insults. In fact, the decrease of ATP content, which reflects the disruption of energy metabolism, and the increase of lipid peroxidation products, which represents oxidative stress, have been observed previously in cocaine-treated mouse liver (55). With regard to the metabolic events associated with decreased fatty acid oxidation, one interesting observation in this study was the lack of change in serum TAG level on day 3 of cocaine treatment in contrast to the dramatic change in hepatic TAG level (Fig. 1C, D), since fatty acids not used for oxidative metabolism in the liver were usually incorporated into TAG and then secreted into the blood via very low density lipoprotein (VLDL) (56). It has been shown that microsomal TAG transfer protein (MTP), which is responsible for assembling VLDL, is inhibited by other known inhibitors of mitochondrial β-oxidation (57). Whether this event contributes to cocaine-induced TAG accumulation and toxicity in the liver requires further investigation.

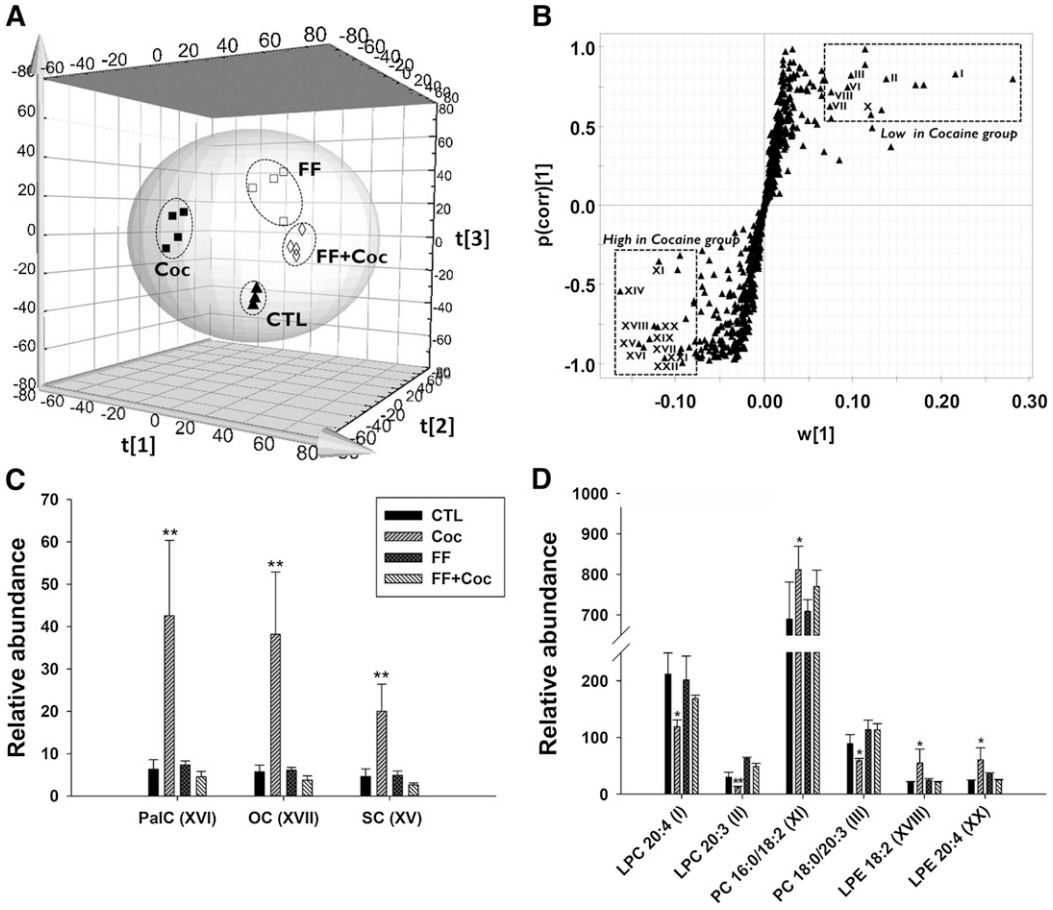

Fig. 7. Influences of fenofibrate on cocaine-induced changes in the lipidome. (A) The three-dimensional scores plot of a PLS-DA model on serum samples from the control mice treated with CMC [labeled as CTL (filled triangle)] and the mice treated with fenofibrate [labeled as FF (open square)], cocaine [labeled as Coc (filled square)] and fenofibrate-cocaine [labeled as FF+Coc (open diamond)]. The $t[1]$, $t[2]$ and $t[3]$ values represent the scores of each sample in the principal component 1, 2, and 3, respectively. Fitness (R^2) and prediction power (Q^2) of this PLS-DA model are 0.91 and 0.72, respectively. (B) The S-loadings plot of serum ions contributing to the distinction of the cocaine-alone treatment from the other three treatment groups. Serum lipid markers identified in Fig. 2B were labeled, and their chemical identities are listed in Table 1. (C) Relative abundance of acylcarnitines in the serum. (D) Relative abundance of LPC, PC, and LPE in the serum. Values were presented as mean ± SD (n = 3–4). $^*P < 0.05$ and $^{**}P < 0.01$ indicate statistical significance between control and marked samples.

Although the exact mitochondrial targets of cocaine in mouse liver was not revealed by this study, a potential cause behind the observation of β-oxidation inhibition on day 3, but not day 1, of cocaine treatment, was revealed by the profiling of urinary cocaine metabolites, which showed that two *N*-oxidative metabolites, norcocaine and benzoylnorecgonine, significantly increased on day 3, whereas the level of benzoylecognine, a hydrolytic product of cocaine, decreased significantly (Fig. 6). It is known that oxidative metabolites of cocaine are responsible for cocaine-induced depression of mitochondrial function and generation of reactive oxygen species (14, 58). Therefore, the correlation of their urinary levels with acylcarnitine levels in serum and liver implied that the increased oxidative metabolism of cocaine might contribute to the cocaine-induced impairment of mitochondrial β-oxidation. Examining the effect of individual cocaine metabolites on acylcarnitine level in future studies will reveal their separate contributions to cocaine-induced lipotoxicity.

The observation of protective effects of fenofibrate cotreatment in this study further confirmed the importance of fatty acid oxidation in cocaine-induced hepatotoxicity (Fig. 5). As an agonist of nuclear receptor PPARα, fenofibrate induced the expression of PPARα-targeted genes (Fig. 9). Concurrent administration of fenofibrate with cocaine treatment abolished the adverse effects of cocaine on TAG turnover, lipid peroxidation, acylcarnitine level, and β-oxidation activity (Figs. 5, 7, and 8) without affecting cocaine metabolism (Fig. 6), which suggests that the regulation of PPARα-mediated pathways, especially fatty acid metabolism, is likely the main mechanism underlying the protective effects of fenofibrate. Fenofibrate and other fibrate compounds have been widely used to treat hypertriglyceridemia in humans. Recently, two clinical studies have reported high TAG levels in the blood and heart of cocaine-dependent human subjects (59, 60). Based on the protective effects of fenofibrate against cocaine-induced hepatotoxicity in this study and the proven

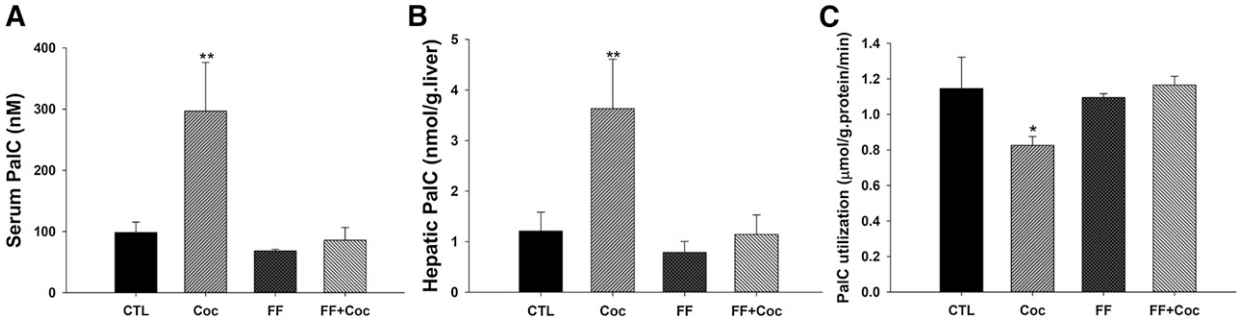

Fig. 8. Protective effects of fenofibrate against cocaine-induced inhibition of fatty acid oxidation function in the liver. (A) PalC level in the serum. (B) PalC level in the liver. (C) Utilization of PalC in the liver. The procedure of in vitro β-oxidation functional assay is described in Experimental Procedures. The utilization of PalC was interpreted as micromoles of PalC that was translocated from the cytosol to the mitochondria of hepatocytes per gram of liver protein per minute. Values were presented as mean ± SD (n = 3–4). $*P < 0.05$ indicates statistical significance between control and marked samples.

beneficial effects of fibrates on dyslipidemia and cardiovascular diseases, it is reasonable to postulate that fibrates might offer hepato- and cardioprotective effects on cocaine users through metabolic modulation of mitochondrial functions. In fact, this potential value of fibrate in the protection against preexisting cocaine toxicity in humans was indicated by the observed partial protective effects from postcocaine administration of fenofibrate in this study (supplementary Fig. VI).

Besides identifying long-chain acylcarnitines as the biomarkers of cocaine-induced hepatotoxicity, LC-MS-based metabolomic and lipidomic analyses of serum and liver in this study revealed dramatic changes in the levels of major phospholipid species, including LPCs, PCs, LPEs, and PEs, as well as the increase of saturated fatty acids and the decrease of PUFAs in the acyl composition of phospholipids (Table 1). Examining the pattern of these time-dependent changes indicated that some lipid species (I, III, VI, XIII, XI, XVIII) were affected immediately after cocaine exposure, whereas others (II, XII, XIX–XXI) were better correlated to the appearance of liver injury (Fig. 3). More importantly, the majority of these changes, together with liver toxicity, were reversed by fenofibrate (Fig. 7C), which suggests their relevance to cocaine-induced toxicities. One interesting observation related to these changes is the similarity to the reported lipidomic changes induced by ethanol exposure (61, 62), such as the decrease of PUFA-comprised lipid species and the imbalance between LPC and LPE species (Fig. 3B, D and Table 1). Another feature of these observed changes in the lipidome is their potential relevance to the functions of PPARα, such as the elongation and desaturation of fatty acids (63). Whether these changes in the lipidome are common events in chemical-induced hepatotoxicity and how PPARα contributes to these changes require further study.

Overall, the combination of LC-MS-based lipidomics, animal modeling, and biochemical analysis in this study enabled the characterization of cocaine-induced dramatic changes in lipid metabolism. The inhibition of mitochondrial fatty acid oxidation was identified as a contributing mechanism of cocaine-induced hepatotoxicity, and the protective effects of fenofibrate suggest a potential strategy in reducing the hepatic side effects of cocaine in clinical settings.

The authors thank the National Institute on Drug Abuse (NIDA) Research Resources Drug Supply Program for providing the cocaine and cocaine metabolites used in this study.

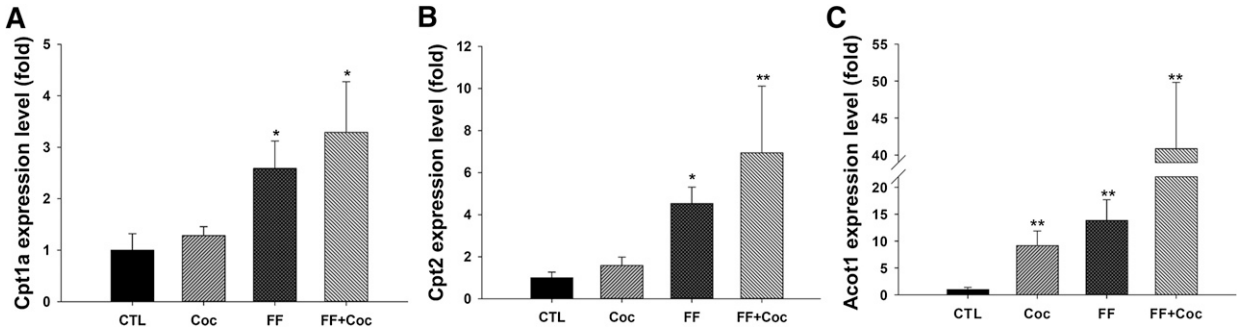

Fig. 9. Expression of PPARα-targeted genes in the liver after cocaine and fenofibrate treatments. (A) *Cpt1a* expression level. (B) *Cpt2* expression level. (C) *Acot1* expression level. The gene expression level of control samples were arbitrarily set as 1. Values were presented as mean ± SD (n = 3–4). $*P < 0.05$ and $**P < 0.01$ indicate statistical significance between control and marked samples.

REFERENCES

1. Nutt, D., L. A. King, W. Saulsbury, and C. Blakemore. 2007. Development of a rational scale to assess the harm of drugs of potential misuse. *Lancet.* **369:** 1047–1053.
2. Laso , W. 2001. Neurochemical and pharmacological aspects of cocaine-induced seizures. *Pol. J. Pharmacol.* **53:** 57–60.
3. Knuepfer, M. M. 2003. Cardiovascular disorders associated with cocaine use: myths and truths. *Pharmacol. Ther.* **97:** 181–222.
4. Cascales, M., A. Alvarez, P. Gasco, L. Fernandez-Simon, N. Sanz, and L. Bosca. 1994. Cocaine-induced liver injury in mice elicits specific changes in DNA ploidy and induces programmed death of hepatocytes. *Hepatology.* **20:** 992–1001.
5. Shuster, L., F. Quimby, A. Bates, and M. L. Thompson. 1977. Liver damage from cocaine in mice. *Life Sci.* **20:** 1035–1041.
6. Jover, R., X. Ponsoda, M. J. Gomez-Lechon, C. Herrero, J. del Pino, and J. V. Castell. 1991. Potentiation of cocaine hepatotoxicity by ethanol in human hepatocytes. *Toxicol. Appl. Pharmacol.* **107:** 526–534.
7. Kothur, R., F. Marsh, and G. Posner. 1991. Liver function tests in nonparenteral cocaine users. *Arch. Intern. Med.* **151:** 1126–1128.
8. Cantilena, L. R., S. A. Cherstniakova, G. Saviolakis, R. Kahn, A. Elkashef, L. Rose, and F. Vocci. 2007. Prevalence of abnormal liver-associated enzymes in cocaine experienced adults versus healthy volunteers during phase 1 clinical trials. *Contemp. Clin. Trials.* **28:** 695–704.
9. Porter, J. M., M. S. Sussman, and G. M. Rosen. 1988. Cocaine-induced hepatotoxicity. *Hepatology.* **8:** 1713.
10. Wanless, I. R., S. Dore, N. Gopinath, J. Tan, R. Cameron, E. J. Heathcote, L. M. Blendis, and G. Levy. 1990. Histopathology of cocaine hepatotoxicity. Report of four patients. *Gastroenterology.* **98:** 497–501.
11. Boelsterli, U. A., and C. Goldlin. 1991. Biomechanisms of cocaine-induced hepatocyte injury mediated by the formation of reactive metabolites. *Arch. Toxicol.* **65:** 351–360.
12. Selim, K., and N. Kaplowitz. 1999. Hepatotoxicity of psychotropic drugs. *Hepatology.* **29:** 1347–1351.
13. Kloss, M. W., G. M. Rosen, and E. J. Rauckman. 1984. Cocaine-mediated hepatotoxicity. A critical review. *Biochem. Pharmacol.* **33:** 169–173.
14. Kovacic, P. 2005. Role of oxidative metabolites of cocaine in toxicity and addiction: oxidative stress and electron transfer. *Med. Hypotheses.* **64:** 350–356.
15. Evans, M. A. 1983. Role of protein binding in cocaine-induced hepatic necrosis. *J. Pharmacol. Exp. Ther.* **224:** 73–79.
16. Masini, A., D. Gallesi, F. Giovannini, T. Trenti, and D. Ceccarelli. 1997. Membrane potential of hepatic mitochondria after acute cocaine administration in rats–the role of mitochondrial reduced glutathione. *Hepatology.* **25:** 385–390.
17. Kloss, M. W., G. M. Rosen, and E. J. Rauckman. 1983. N-demethylation of cocaine to norcocaine. Evidence for participation by cytochrome P-450 and FAD-containing monooxygenase. *Mol. Pharmacol.* **23:** 482–485.
18. Zimmerman, E. F., R. B. Potturi, E. Resnick, and J. E. Fisher. 1994. Role of oxygen free radicals in cocaine-induced vascular disruption in mice. *Teratology.* **49:** 192–201.
19. Vergeade, A., P. Mulder, C. Vendeville-Dehaudt, F. Estour, D. Fortin, R. Ventura-Clapier, C. Thuillez, and C. Monteil. 2010. Mitochondrial impairment contributes to cocaine-induced cardiac dysfunction: prevention by the targeted antioxidant MitoQ. *Free Radic. Biol. Med.* **49:** 748–756.
20. Dietrich, J. B., A. Mangeol, M. O. Revel, C. Burgun, D. Aunis, and J. Zwiller. 2005. Acute or repeated cocaine administration generates reactive oxygen species and induces antioxidant enzyme activity in dopaminergic rat brain structures. *Neuropharmacology.* **48:** 965–974.
21. Nicholson, J. K., and I. D. Wilson. 2003. Opinion: understanding 'global' systems biology: metabonomics and the continuum of metabolism. *Nat. Rev. Drug Discov.* **2:** 668–676.
22. Chen, C., F. J. Gonzalez, and J. R. Idle. 2007. LC-MS-based metabolomics in drug metabolism. *Drug Metab. Rev.* **39:** 581–597.
23. Johnson, C. H., and F. J. Gonzalez. 2012. Challenges and opportunities of metabolomics. *J. Cell Physiol.* **227:** 2975–2981.
24. Sreekumar, A., L. M. Poisson, T. M. Rajendiran, A. P. Khan, Q. Cao, J. Yu, B. Laxman, R. Mehra, R. J. Lonigro, Y. Li, et al. 2009. Metabolomic profiles delineate potential role for sarcosine in prostate cancer progression. *Nature.* **457:** 910–914.
25. Chen, C., Y. M. Shah, K. Morimura, K. W. Krausz, M. Miyazaki, T. A. Richardson, E. T. Morgan, J. M. Ntambi, J. R. Idle, and F. J. Gonzalez. 2008. Metabolomics reveals that hepatic stearoyl-CoA desaturase 1 downregulation exacerbates inflammation and acute colitis. *Cell Metab.* **7:** 135–147.
26. Shi, X., D. Yao, and C. Chen. 2012. Identification of N-acetyltaurine as a novel metabolite of ethanol through metabolomics-guided biochemical analysis. *J. Biol. Chem.* **287:** 6336–6349.
27. Patkar, A. A., S. Rozen, P. Mannelli, W. Matson, C. U. Pae, K. R. Krishnan, and R. Kaddurah-Daouk. 2009. Alterations in tryptophan and purine metabolism in cocaine addiction: a metabolomic study. *Psychopharmacology (Berl.).* **206:** 479–489.
28. Wiener, H. L., and M. E. Reith. 1990. Differential effects of daily administration of cocaine on hepatic and cerebral glutathione in mice. *Biochem. Pharmacol.* **40:** 1763–1768.
29. Janero, D. R. 1990. Malondialdehyde and thiobarbituric acid-reactivity as diagnostic indices of lipid peroxidation and peroxidative tissue injury. *Free Radic. Biol. Med.* **9:** 515–540.
30. Bligh, E. G., and W. J. Dyer. 1959. A rapid method of total lipid extraction and purification. *Can. J. Biochem. Physiol.* **37:** 911–917.
31. Bylesjö, M., M. Rantalainen, O. Cloarec, J. K. Nicholson, E. Holmes, and J. Trygg. 2006. OPLS discriminant analysis: combining the strengths of PLS-DA and SIMCA classification. *J. Chemometr.* **20:** 341–351.
32. Brady, L. J., and C. L. Hoppel. 1983. Effect of diet and starvation on hepatic mitochondrial function in the rat. *J. Nutr.* **113:** 2129–2137.
33. Vatamaniuk, M. Z., O. V. Horyn, O. K. Vatamaniuk, and N. M. Doliba. 2003. Acetylcholine affects rat liver metabolism via type 3 muscarinic receptors in hepatocytes. *Life Sci.* **72:** 1871–1882.
34. Chen, C., X. Ma, M. A. Malfatti, K. W. Krausz, S. Kimura, J. S. Felton, J. R. Idle, and F. J. Gonzalez. 2007. A comprehensive investigation of 2-amino-1-methyl-6-phenylimidazo[4,5-b]pyridine (PhIP) metabolism in the mouse using a multivariate data analysis approach. *Chem. Res. Toxicol.* **20:** 531–542.
35. Desvergne, B., L. Michalik, and W. Wahli. 2006. Transcriptional regulation of metabolism. *Physiol. Rev.* **86:** 465–514.
36. van Raalte, D. H., M. Li, P. H. Pritchard, and K. M. Wasan. 2004. Peroxisome proliferator-activated receptor (PPAR)-alpha: a pharmacological target with a promising future. *Pharm. Res.* **21:** 1531–1538.
37. Martin, P. G., H. Guillou, F. Lasserre, S. Dejean, A. Lan, J. M. Pascussi, M. Sancristobal, P. Legrand, P. Besse, and T. Pineau. 2007. Novel aspects of PPARalpha-mediated regulation of lipid and xenobiotic metabolism revealed through a nutrigenomic study. *Hepatology.* **45:** 767–777.
38. Thompson, M. L., L. Shuster, and K. Shaw. 1979. Cocaine-induced hepatic necrosis in mice–the role of cocaine metabolism. *Biochem. Pharmacol.* **28:** 2389–2395.
39. Ndikum-Moffor, F. M., T. R. Schoeb, and S. M. Roberts. 1998. Liver toxicity from norcocaine nitroxide, an N-oxidative metabolite of cocaine. *J. Pharmacol. Exp. Ther.* **284:** 413–419.
40. Galloway, M. P. 1988. Neurochemical interactions of cocaine with dopaminergic systems. *Trends Pharmacol. Sci.* **9:** 451–454.
41. Young, J. B., and L. Landsberg. 1977. Catecholamines and intermediary metabolism. *Clin. Endocrinol. Metab.* **6:** 599–631.
42. Barth, E., G. Albuszies, K. Baumgart, M. Matejovic, U. Wachter, J. Vogt, P. Radermacher, and E. Calzia. 2007. Glucose metabolism and catecholamines. *Crit. Care Med.* **35:** S508–S518.
43. Vaughan, M. 1966. Second symposium on catecholamines. Lipid metabolism. Introductory remarks. *Pharmacol. Rev.* **18:** 215–216.
44. Wenke, M. 1966. Effects of catecholamines on lipid metabolism. *Adv. Lipid Res.* **4:** 69–105.
45. Lundholm, L., and E. Mohme-Lundholm. 1959. The effect of cocaine and adrenaline on blood lactic acid and oxygen consumption in rabbits. *Acta Pharmacol. Toxicol. (Copenh.).* **15:** 257–264.
46. Ojuka, E. O., J. D. Bell, G. W. Fellingham, and R. K. Conlee. 1996. Cocaine and exercise: alteration in carbohydrate metabolism in adrenodemedullated rats. *J. Appl. Physiol.* **80:** 124–132.
47. Tuncel, M., Z. Wang, D. Arbique, P. J. Fadel, R. G. Victor, and W. Vongpatanasin. 2002. Mechanism of the blood pressure–raising effect of cocaine in humans. *Circulation.* **105:** 1054–1059.
48. MacLachlan, P. L., and H. C. Hodge. 1939. The influence of cocaine feeding on the liver lipids of the white mouse. *J. Biol. Chem.* **127:** 721–726.
49. Odeleye, O. E., M. C. Lopez, B. T. Smith, C. D. Eskelson, and R. R. Watson. 1992. Cocaine hepatotoxicity during protein undernutrition of retrovirally infected mice. *Can. J. Physiol. Pharmacol.* **70:** 338–343.

50. Rajab, R., E. Stearns, and S. Baithun. 2008. Autopsy pathology of cocaine users from the Eastern district of London: a retrospective cohort study. *J. Clin. Pathol.* **61:** 848–850.
51. Gottfried, M. R., M. W. Kloss, D. Graham, E. J. Rauckman, and G. M. Rosen. 1986. Ultrastructure of experimental cocaine hepatotoxicity. *Hepatology.* **6:** 299–304.
52. Weinberg, G. L., R. Ripper, S. Bern, B. Lin, L. Edelman, G. Digregorio, M. Piano, and D. L. Feinstein. 2011. Pioglitazone attenuates acute cocaine toxicity in rat isolated heart: potential protection by metabolic modulation. *Anesthesiology.* **114:** 1389–1395.
53. Chen, C., K. W. Krausz, Y. M. Shah, J. R. Idle, and F. J. Gonzalez. 2009. Serum metabolomics reveals irreversible inhibition of fatty acid beta-oxidation through the suppression of PPARalpha activation as a contributing mechanism of acetaminophen-induced hepatotoxicity. *Chem. Res. Toxicol.* **22:** 699–707.
54. Fromenty, B., and D. Pessayre. 1995. Inhibition of mitochondrial beta-oxidation as a mechanism of hepatotoxicity. *Pharmacol. Ther.* **67:** 101–154.
55. Devi, B. G., and A. W. Chan. 1996. Cocaine-induced peroxidative stress in rat liver: antioxidant enzymes and mitochondria. *J. Pharmacol. Exp. Ther.* **279:** 359–366.
56. Havel, R. J. 2010. Triglyceride-rich lipoproteins and plasma lipid transport. *Arterioscler. Thromb. Vasc. Biol.* **30:** 9–19.
57. Lettéron, P., A. Sutton, A. Mansouri, B. Fromenty, and D. Pessayre. 2003. Inhibition of microsomal triglyceride transfer protein: another mechanism for drug-induced steatosis in mice. *Hepatology.* **38:** 133–140.
58. Boess, F., F. M. Ndikum-Moffor, U. A. Boelsterli, and S. M. Roberts. 2000. Effects of cocaine and its oxidative metabolites on mitochondrial respiration and generation of reactive oxygen species. *Biochem. Pharmacol.* **60:** 615–623.
59. Sáez, C. G., P. Olivares, J. Pallavicini, O. Panes, N. Moreno, T. Massardo, D. Mezzano, and J. Pereira. 2011. Increased number of circulating endothelial cells and plasma markers of endothelial damage in chronic cocaine users. *Thromb. Res.* **128:** e18–e23.
60. Liu, C., A. Redheuil, R. Ouwerkerk, J. Lima, D. Bluemke, and S. Lai. 2010. Cocaine use as an independent predictor of cardiac steatosis: initial experience by 1H spectroscopy. *J. Cardiovasc. Magn. Reson.* **12(Suppl. 1):** O90.
61. Clugston, R. D., H. Jiang, M. X. Lee, R. Piantedosi, J. J. Yuen, R. Ramakrishnan, M. J. Lewis, M. E. Gottesman, L. S. Huang, I. J. Goldberg, et al. 2011. Altered hepatic lipid metabolism in C57BL/6 mice fed alcohol: a targeted lipidomic and gene expression study. *J. Lipid Res.* **52:** 2021–2031.
62. Lieber, C. S., S. J. Robins, and M. A. Leo. 1994. Hepatic phosphatidylethanolamine methyltransferase activity is decreased by ethanol and increased by phosphatidylcholine. *Alcohol. Clin. Exp. Res.* **18:** 592–595.
63. Wang, Y., D. Botolin, J. Xu, B. Christian, E. Mitchell, B. Jayaprakasam, M. G. Nair, J. M. Peters, J. V. Busik, L. K. Olson, et al. 2006. Regulation of hepatic fatty acid elongase and desaturase expression in diabetes and obesity. *J. Lipid Res.* **47:** 2028–2041.